MCB
Journals.ASM.org

KSRP and MicroRNA 145 Are Negative Regulators of Lipolysis in White Adipose Tissue

Yi-Yu Lin,[a] Chu-Fang Chou,[a] Matteo Giovarelli,[b] Paola Briata,[b] Roberto Gherzi,[b] Ching-Yi Chen[a]

Department of Biochemistry & Molecular Genetics, University of Alabama at Birmingham, Birmingham, Alabama, USA[a]; Gene Expression Regulation Laboratory, IRCCS AOU San Martino-IST, Genoa, Italy[b]

White adipose tissue (WAT) releases fatty acids from stored triacylglycerol for an energy source. Here, we report that targeted deletion of KH-type splicing regulatory protein (KSRP), an RNA-binding protein that regulates gene expression at multiple levels, enhances lipolysis in epididymal WAT (eWAT) because of the upregulation of genes promoting lipolytic activity. Expression of microRNA 145 (miR-145) is decreased because of impaired primary miR-145 processing in *Ksrp*$^{-/-}$ eWAT. We show that miR-145 directly targets and represses *Foxo1* and *Cgi58*, activators of lipolytic activity, and forced expression of miR-145 attenuates lipolysis. This study reveals a novel *in vivo* function of KSRP in controlling adipose lipolysis through posttranscriptional regulation of miR-145 expression.

Nutrients providing excess calories are converted to triacylglycerol (TAG) for storage in lipid droplets of white adipose tissue (WAT). The stored TAG is hydrolyzed to release fatty acids, which are crucial for energy production in muscle and other organs during times of demand such as fasting or exercise (1). However, excess TAG accumulation in WAT results in obesity, which increases the risk of diabetes, heart disease, and some forms of cancer. The content of TAG in WAT is determined by the balance of anabolic (esterification of glycerol with fatty acids) and catabolic (lipolytic reactions that hydrolyze TAG to glycerol and fatty acids, referred to as lipolysis) pathways. While the hydrolysis of stored TAG is crucial for providing energy, recent studies have demonstrated that increasing lipolysis in WAT causes an elevation in fatty acid utilization and energy expenditure, thereby protecting against obesity (2, 3). Thus, understanding the regulation of lipolysis in WAT and identification of factors that control this activity may be crucial for the development of therapeutics to prevent obesity and its related disorders.

Three adipocyte lipases are involved in sequential lipolytic reactions and include adipose triglyceride lipase (ATGL) encoded by *Pnpla2*, hormone-sensitive lipase (HSL) encoded by *Lipe*, and monoglyceride lipase. ATGL cleaves TAG (4–6), HSL converts diacylglycerol to monoacylglycerol (7), and monoglyceride lipase catalyzes the final step of lipolysis. Lipolysis is tightly controlled by hormones that are secreted according to nutritional status. During fasting, catecholamines bind to β-adrenergic receptors, leading to elevation of cyclic AMP levels and activation of protein kinase A, resulting in stimulation of lipolysis. In contrast, in the fed state, lipolysis is inhibited by insulin (1). In addition to hormones, additional regulators also play critical roles in controlling lipolysis. Transcriptional activation of *Pnpla2* by forkhead box O1 (FOXO1) and interferon regulatory factor 4 enhances lipolysis in adipocytes (8, 9). ATGL interacts with regulatory proteins that activate or attenuate its enzyme activity, in which CGI58 (comparative gene identification 58, also referred to as alpha/beta hydrolase domain 5, ABHD5) serves as a coactivator of ATGL activity (10), and G0S2 (G_0-G_1 switch gene 2) serves as an inhibitor of ATGL (11).

KSRP is a multifunctional RNA-binding protein involved in the posttranscriptional regulation of gene expression, including splicing (12), mRNA decay (13), primary microRNA (pri-miRNA) processing (14), and translation (15). KSRP binds the AU-rich elements (AREs) in the 3′ untranslated regions (UTRs) of inherently unstable mRNAs and promotes their decay by recruiting mRNA decay machineries (13, 16). It also interacts with the terminal loops of a subset of miRNA precursors and promotes their maturation in cultured cells (14). However, the *in vivo* function of KSRP in controlling pri-miRNA processing has not been completely established. To do this, we have generated *Ksrp*-null mice (17). Here, we report that lipolysis is elevated in *Ksrp*$^{-/-}$ eWAT because of enhanced expression of *Pnpla2*, *Lipe*, *Foxo1*, and *Cgi58* and expression of miRNA 145 (miR-145) is decreased because of impaired pri-miR-145 processing. Using 3T3-L1 adipocytes, we demonstrate that miR-145 represses lipolysis by targeting *Foxo1* and *Cgi58* and downregulation of *Foxo1* and *Cgi58* attenuates lipolysis. Thus, these findings establish KSRP and miR-145 as important negative regulators of lipolysis in WAT.

MATERIALS AND METHODS

Animal studies. Generation of *Ksrp*-null mice in a C57BL/6J background has been described previously (17). Mice were maintained under a 12-h light–12-h dark cycle. All experiments were performed with 10- to 16-week-old male mice. All animal studies were conducted in accordance with the guidelines for animal use and care established by the University of Alabama at Birmingham Animal Resource Program and the Institutional Animal Care and Use Committee.

Isolation of adipocytes and lipolysis assay. Primary adipocytes were isolated from epididymal fat depots by collagenase digestion as described previously (18). Briefly, fat pads were rinsed with phosphate-buffered saline (PBS), minced, and digested for 45 min at 37°C in Krebs-Ringer-HEPES (KRH) buffer (121 mM NaCl, 4.9 mM KCl, 1.2 mM $MgSO_4$, 0.33 mM $CaCl_2$, 12 mM HEPES, pH 7.4) containing 3% bovine serum albumin

Received 9 January 2014 Returned for modification 28 January 2014
Accepted 6 April 2014
Published ahead of print 14 April 2014
Address correspondence to Ching-Yi Chen, cchen@uab.edu.

doi:10.1128/MCB.00042-14

TABLE 1 Real-time PCR primers used in this study

Primer	Sequence	
	Forward	Reverse
β-Actin	GTTCCGATGCCCTGAGGCTC	CAGACAGCACTGTGTTGGCA
Acadl	TCTGGACTCCGGTTCTGCTTC	TCTGTCTTGCGATCAGCTCTT
Acadm	AGACGAAGCCACGAAGTATGC	TCATCAGCTTCTCCACAGGGT
Cebpa	GGTGGACAAGAACAGCAACGA	TGTCCAGTTCACGGCTCAGCT
Cgi58	ACGATTCCTTATGGGTGGGCC	ACACATAATGCCCCGCCCCGA
Cidea	CTTCCTCGGCTGTCTCAATGT	GGGGGATGGCTGCTCTTCTGT
Cox8b	CTCCCCCCTATCCTGCGGCTG	ACTATGGCTGAGATCCCCACA
Cyclophilin B	AAGGTGCTCTTCGCCGCCGCC	TGATGACACGATGGAACTTGCTGT
Fabp4	ATGCCTTTGTGGGAACCTGGA	TCACCTTCCTGTCGTCTGCGG
Foxo1	GTGGATGGTGAAGAGCGTGCC	TTCCGCTCTTGCCTCCCTCTG
G0S2	CCTCTCTTCCCACTGCACCCT	GGCTGGCGGCTGTGAAAGGGC
Irf4	AGCTAGAAAGAGACCAGACTTGCA	TGGAGTGGTAACGTGTTCAGGTAA
Lipe	CACAGAGACACCAGCCAACG	CACTCCTGGTCGGTTGATGG
Plin2	ACGACGACACCGATGAGTCCC	GTGAGGACGCCATCGGACACT
Pnpla2	ACGCCACTCACATCTACGGA	CAATCAGCAGGCAGGGTCTT
Ppara	GGCTGCTATAATTTGCTGTGGAG	TGTGTACGAGCTGCGCATGC
Pparg	TGCGGAAGCCCTTTGGTGACT	ATGTCCTCGATGGGCTTCACGTTC
Ppard	CCGCAAGCCCTTCAGTGACATCAT	GCAGATGGAATTCTAGAGCCCGCA
Ppargc1a	TCATCACCTACCGTTACACCT	TATCAAAATCCAGAGAGTCAT
Prdm16	AGTCGGACAACCATGCACTTT	TCCTTGGGGCTCAGGTGTGGG
Pri-miR-145 Expression	P1: GGTGGCTGCTGGGACTTGAAC	P2: GGGTCAGGAGCCAGCATGAAG
Pri-miR-145 Expression	P3: GAGTGCAAAGGATGGGCGAGC	P4: CTCCCCTGTTTGTGCCCCGCC
Pri-miR-145 RIP	CCCTCCTGGGGATGTTAGGA	CGGTCTTGGGAGCTCTCTTC
Ucp1	CACCTTCCCGCTGGACACT	CCCTAGGACACCTTTATACCTAATGG

(BSA) and 1.5 mg/ml type I collagenase. The digested tissues were filtered through a 500-μm metal mesh and centrifuged at 500 × *g* for 5 min. The floating adipocytes were collected and washed with KRH buffer. Primary adipocytes (1×10^5 cells/ml), tissue explants (~100 mg), and 3T3-L1 adipocytes were incubated with KRH buffer containing 3% fatty acid-free BSA in the absence or presence of 1 μM isoproterenol at 37°C. The amounts of glycerol and fatty acid (FA) released were determined with free-glycerol reagent (Sigma) and a fatty acid kit (Sigma), respectively.

Measurement of adipocyte numbers and TAG contents. Adipocyte numbers were determined with a hemocytometer. Lipids were extracted from adipocytes in 1% Triton X-100, and TAG contents were determined with Infinity reagent (Thermo Scientific).

Measurement of adipocyte sizes. Epididymal WATs were fixed in PBS containing 10% formalin and embedded in paraffin. Tissue sections were stained with hematoxylin and eosin. Five separate fields were selected for each mouse, and adipocyte sizes were determined with ImageJ software.

mRNA analysis. Total RNA was extracted by TRIzol (Invitrogen). For quantitative real-time RT-PCR analysis, total RNA (1 μg) was reverse transcribed with a mixture of oligo(dT) and random hexamers. Amplification was performed with the Roche LC480 LightCycler and SYBR green system (Roche). mRNA levels were normalized to that of β-actin or cyclophilin mRNA. The sequences of the primers used are listed in Table 1.

miRNA microarrays and analysis. RNA was isolated from eWATs of six wild-type and six *Ksrp*$^{-/-}$ mutant mice by miRNeasy (Qiagen). Individual RNAs of wild-type and *Ksrp*$^{-/-}$ mice, respectively, were pooled and subjected to genome-wide miRNA microarray analysis in triplicate performed by Phalanx Biotech. The signals of miRNAs that were 5-fold above the background (these are arbitrarily considered to be expressed in eWAT) and elevated >2-fold in *Ksrp*$^{-/-}$ eWAT were selected for further analysis. For miR-145 expression analysis, total RNA was converted into cDNA with the miScript II RT kit (Qiagen) and subjected to real-time PCR with a specific primer for miR-145 by using the miScript Primer Assay (Qiagen). miRNA levels were normalized to that of U6 snRNA.

miRNA target prediction. miRNA target prediction was performed by using the miRWalk database (http://www.umm.uni-heidelberg.de/apps/zmf/mirwalk/).

Pri-miRNA *in vitro* processing assay. A DNA template producing pri-miR-145 was generated by PCR. ^{32}P-labeled pri-miR-145 was synthesized by *in vitro* transcription and incubated with total extracts of wild-type and *Ksrp*$^{-/-}$ eWATs in a processing buffer. Pri-miRNA processing assays were performed as described previously (14, 19).

RIP assays. Ribonucleoprotein immunoprecipitation (RIP) assays were performed as described previously (19, 20). Immunoprecipitated pellets were washed, and RNA was isolated, reverse transcribed, and amplified by quantitative PCR (qPCR).

Immunoblotting and antibodies. Proteins were separated by 10% SDS-PAGE and transferred to a polyvinylidene difluoride membrane, which was probed with anti-FOXO1 (Cell Signaling), anti-CGI58 (Abcam), anti-ATGL (Cell Signaling), anti-KSRP (21), anti-α-tubulin (Sigma), and anti-β-actin (Abcam) antibodies.

Cell culture and transfection. 3T3-L1 preadipocytes were purchased from the American Type Culture Collection and maintained in Dulbecco's modified Eagle's medium (DMEM) with 10% bovine calf serum (BCS). 3T3-L1 cells were plated in 12-well plates at a density of 80 to 90% confluence and transfected with small interfering RNAs (siRNAs; 60 nM), miRNA mimics (50 nM), or plasmid DNA (1 μg) with 4 μl of Lipofectamine (Invitrogen) in 500 μl of Opti-MEM (Invitrogen) for 6 h the following day. The transfected cells were incubated with DMEM containing 10% BCS for 40 h and induced for differentiation by incubation with DMEM containing 10% FBS, 5 μg/ml insulin, 0.5 mM isobutylmethylxanthine, and 1 μM dexamethasone for 2 days. The transfected cells were transfected with the same siRNA, miRNA, or plasmid again as in the first transfection in Opti-MEM for 6 h. Cells then were cultured in DMEM containing 10% FBS and 5 μg/ml insulin and collected for analysis 5 days after the induction of adipogenesis. For lipolytic gene expression, adipocytes were serum starved for 16 h and stimulated with 1 μM isoproterenol for 2 h. Mouse embryonic fibroblasts (MEFs) were prepared (17),

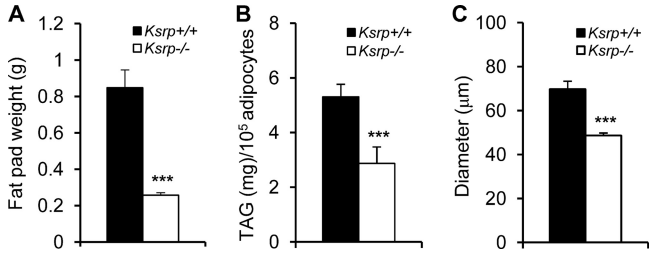

FIG 1 KSRP ablation causes a reduction in fat pad weight, TAG content, and adipocyte size. (A) Epididymal fat pad weights of 14-week-old wild-type ($n = 8$) and $Ksrp^{-/-}$ mutant ($n = 8$) male mice. (B) TAG contents of adipocytes isolated from eWAT of 12-week-old wild-type ($n = 4$) and $Ksrp^{-/-}$ ($n = 4$) mice. (C) Average diameters of adipocytes determined by hematoxylin-and-eosin staining of paraffin-embedded sections of eWAT of wild-type and $Ksrp^{-/-}$ mice. Results were obtained from three wild-type and three $Ksrp^{-/-}$ mice and ~150 adipocytes per mouse. All data are presented as mean ± SEM. ***, $P < 0.001$.

differentiated to adipocytes, and harvested at day 8 for RNA extraction, as well as Oil Red O staining as described previously (22).

Luciferase reporters and assay. Dual-luciferase reporters, expressing firefly and *Renilla* luciferases and containing the 3′ UTRs of *Foxo1* and *Cgi58* subcloned downstream of firefly luciferase, and a control reporter, pEZX-MT01, were purchased from GeneCopoeia. The predicted miR-145 target sites were mutated by PCR-mediated site-directed mutagenesis, and mutations were confirmed by DNA sequencing. NIH 3T3 cells were transfected with 250 ng of reporter together with 50 nM miRNA mimic with Lipofectamine. Cells were collected 36 to 48 h after transfection with Luc-Pair miR luciferase assay kits (GeneCopoeia).

miRNA mimics, siRNAs, and plasmid. miR-145 mimic and SiGENOME SMART pool siRNAs against *Foxo1* and *Cgi58* were purchased from Thermo Scientific. Control miRNA mimic and siRNA were purchased from Qiagen. A plasmid expressing FLAG-KSRP was described previously (17).

Statistical analysis. All data are presented as the mean ± the standard error of the mean (SEM). Statistical significance (*P* value) was calculated by unpaired two-tailed Student *t* test.

RESULTS

KSRP ablation causes a reduction in adiposity resulting from decreased TAG content but not impaired adipocyte differentiation. To determine the *in vivo* function of KSRP, we had previously generated $Ksrp^{-/-}$ mice and found that they had a reduced epididymal fat depot on a chow diet (Fig. 1A). Reduction in adipose tissue mass can result from less TAG storage, impaired adipocyte differentiation, or both. We isolated primary adipocytes from eWAT and determined the total TAG content, which was significantly reduced in $Ksrp^{-/-}$ eWAT (Fig. 1B). Consistent with a decrease in TAG content, adipocytes of $Ksrp^{-/-}$ eWAT were smaller, with a 30% decrease in the mean diameter (Fig. 1C).

To determine whether the reduced adiposity also results from impaired adipocyte differentiation, we examined the expression of adipocyte markers in eWAT of wild-type and $Ksrp^{-/-}$ mice and found no difference in the expression of *Pparg* and *Cebpa*, adipogenic transcriptional factors, and *Fasn*, *Fabp4*, and *Plin2*, late adipocyte markers, between the two groups (Fig. 2A). We next examined whether KSRP deficiency affects the adipocyte differentiation of MEFs. Deletion of KSRP did not alter adipocyte differentiation revealed by Oil Red O staining (Fig. 2B), and no difference in the expression of *Pparg*, *Cebpa*, *fabp4*, and *Plin2* was detected between wild-type and $Ksrp^{-/-}$ MEFs (Fig. 2C). Altogether, these data suggest that KSRP ablation causes a reduction in TAG content and a smaller adipocyte size in WAT, rather than impaired adipocyte differentiation.

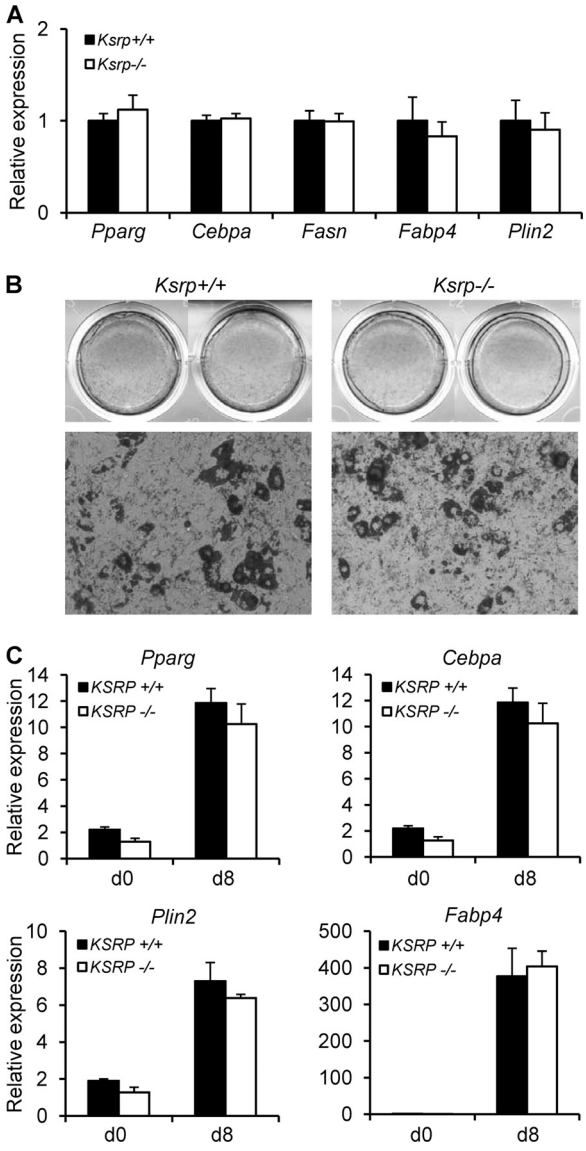

FIG 2 KSRP ablation does not affect adipocyte differentiation. (A) Expression of adipocyte markers, including *Pparg*, *Cebpa*, *Fasn*, *Fabp4*, and *Plin2*, in eWAT of wild-type ($n = 8$) and $Ksrp^{-/-}$ ($n = 8$) mice. The expression of each gene in wild-type mice was set at 1. (B) Wild-type and $Ksrp^{-/-}$ MEFs were induced for adipogenesis for 8 days. Adipocytes were stained with Oil Red O. Two different wild-type and $Ksrp^{-/-}$ MEFs were used. (C) Expression of *Pparg*, *Cebpa*, *Fabp4*, and *Plin2* was analyzed in wild-type and $Ksrp^{-/-}$ MEFs ($n = 4$) before differentiation (d0) and 8 days (d8) after differentiation. All data are presented as mean ± SEM.

KSRP ablation increases lipolysis and expression of genes involved in fatty acid utilization. A plausible mechanism that leads to reduced TAG content in $Ksrp^{-/-}$ eWAT is enhanced lipolysis. We examined the expression of genes involved in lipolysis in eWAT under fed and fasting conditions. The expression of genes that stimulate lipolysis, including *Pnpla2*, *Lipe*, *Foxo1*, *Irf4*, and *Cgi58*, was greater in $Ksrp^{-/-}$ mutant than in wild-type eWAT under both fed and fasting conditions (Fig. 3A). In contrast, no

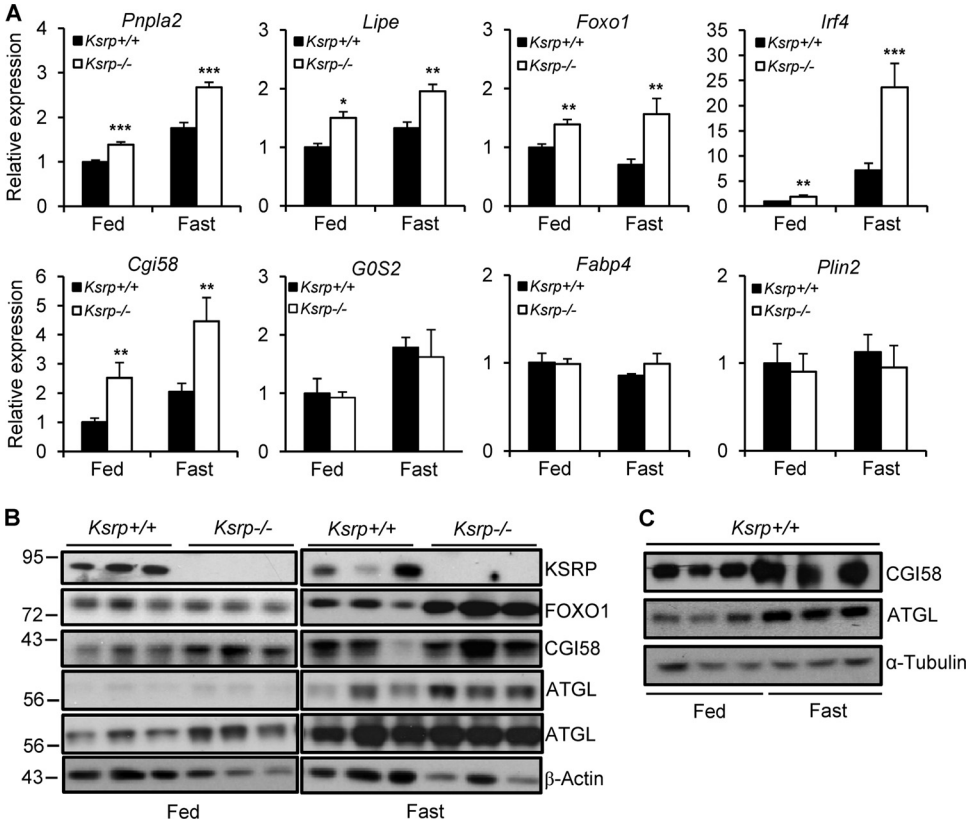

FIG 3 Enhanced expression of genes that stimulate lipolytic activity in *Ksrp*$^{-/-}$ eWAT. (A) Expression of *Pnpla2*, *Lipe*, *Foxo1*, *Irf4*, *Cgi58*, *G0S2*, *Fabp4*, and *Plin2* was analyzed by qPCR in eWAT of fed or 16-h-fasted wild-type ($n = 8$) and *Ksrp*$^{-/-}$ ($n = 8$) mice. The expression of each gene in fed wild-type eWAT was set at 1. Data are mean ± SEM. *, $P < 0.05$; **, $P < 0.01$; ***, $P < 0.001$. (B) Immunoblot analysis of eWAT extracts from fed or fasted wild-type and *Ksrp*$^{-/-}$ mice with antibodies against KSRP, FOXO1, CGI58, ATGL, and β-actin. Two different exposures for ATGL are shown. (C) Fasting induces CGI58 and ATGL. eWAT extracts of fed and fasted wild-type mice were separated on a gel and subjected to immunoblotting with antibodies against CGI58, ATGL, and α-tubulin. The values to the left of panel B are molecular sizes in kilodaltons.

difference in the expression of *G0S2*, *Fabp4*, or *Plin2* was detected between the groups (Fig. 3A). The levels of the FOXO1, CGI58, and ATGL proteins were also significantly increased in *Ksrp*$^{-/-}$ mutant eWAT under both fed and fasting conditions (Fig. 3B). The results in Fig. 3B suggested that fasting induced CGI58 and ATGL in wild-type eWAT. However, these samples were analyzed on different blots although immunoblotting was performed at the same time with the same exposure time for each antibody. To further examine whether CGI58 and ATGL are subject to regulation by nutritional states, we repeated the immunoblotting and analyzed their levels in wild-type eWAT on the same blot under fed and fasting conditions. As shown in Fig. 3C, fasting strongly induced CGI58 and ATGL. To correlate gene expression with lipolytic activity, we measured the lipolysis of isolated adipocytes and tissue explants from wild-type and *Ksrp*$^{-/-}$ mutant eWAT. Glycerol and FA release were elevated in *Ksrp*$^{-/-}$ mutant adipocytes (Fig. 4A and B) and *Ksrp*$^{-/-}$ mutant eWAT (Fig. 4C and D) under both basal and isoproterenol-stimulated conditions.

Recent studies have shown that increasing lipolysis also facilitates FA utilization within WAT (2, 3, 23). Consistent with these previous findings, we observed the upregulation of genes involved in thermogenesis and FA oxidation, including *Ucp1*, *Cidea*, *Cox8b*, *Acadm*, *Acadl*, *Prdm16*, *Ppara*, *Ppard*, and *Ppargc1a*, in *Ksrp*$^{-/-}$ eWAT (Fig. 5). These data indicate that KSRP ablation enhances lipolysis, as well as fat utilization, in eWAT through the upregulation of genes that stimulate lipolysis and mitochondrial FA oxidation.

Reduced miR-145 expression in *Ksrp*$^{-/-}$ eWAT because of impaired pri-miRNA processing. One of the functions of KSRP is to facilitate the processing of a subset of miRNAs. To determine whether impaired expression of miRNAs plays a role in enhancing lipolysis in *Ksrp*$^{-/-}$ eWAT, we subjected RNA samples to miRNA microarray analysis and selected miRNAs whose expression was reduced in the absence of KSRP. We identified only one miRNA, miR-145, whose expression was reduced by >2-fold in *Ksrp*$^{-/-}$ eWAT (see Materials and Methods). We examined miR-145 and pri-miR-145 levels by real-time qPCR and found a decrease in miR-145 levels in *Ksrp*$^{-/-}$ eWAT under both fed and fasting conditions (Fig. 6A). Fasting increased the levels of miR-145 in wild-type eWAT, but the increase was blunted in *Ksrp*$^{-/-}$ eWAT (Fig. 6A). In contrast, pri-miR-145 levels (detected with primers P1 and P2, located immediately downstream of pre-miR-145 and shown in Fig. 6B) were increased in *Ksrp*$^{-/-}$ eWAT under both fed and fasting conditions (Fig. 6C).

To examine whether KSRP regulates the transcription of pri-miR-145, we performed qPCR analysis with primers located in different regions of pri-miR-145. miR-143 and miR-145 are derived from the same bicistronic transcript and are separated by 1.4

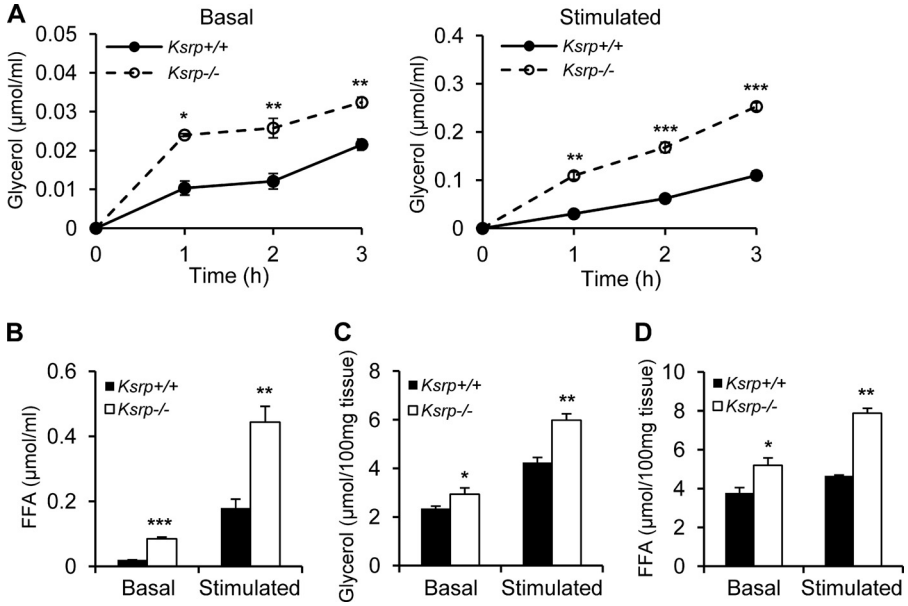

FIG 4 Enhanced lipolysis in *Ksrp*$^{-/-}$ eWAT. (A and B) Glycerol (A) and FA (B) release was measured with equal number of adipocytes (1×10^5 cells/ml) of wild-type or *Ksrp*$^{-/-}$ eWAT in the absence or presence of isoproterenol at different time points (A) or at 3 h (B). (C and D) Glycerol (C) and FA (D) release was measured with wild-type and *Ksrp*$^{-/-}$ eWAT explants in the absence or presence of isoproterenol for 3 h. Data are mean ± SEM. *, $P < 0.05$; **, $P < 0.01$; ***, $P < 0.001$. FFA, free FA.

kb (Fig. 6B). We found that pri-miR-143 and miR-145 transcript levels detected by primers P3 and P4 (located ~300 nucleotides upstream of pre-miR-143) were similar between wild-type and *Ksrp*$^{-/-}$ under both fed and fasting conditions (Fig. 6D). Similar results were obtained with primers located between pre-miR-143 and pre-miR-145 (data not shown). In addition, we observed no difference in the levels of miR-143 between wild-type and *Ksrp*$^{-/-}$ eWAT (data not shown). Altogether, these results suggest that the transcription of pri-miR-143 and miR-145 is unlikely to be altered in *Ksrp*$^{-/-}$ eWAT and KSRP regulates miR-145 but not miR-143 expression at the posttranscriptional level.

To support this, we performed RIP assays and observed that KSRP physically associated with pri-miR-145 in wild-type eWAT extracts (Fig. 6E). *In vitro* pri-miRNA processing assays showed that production of pre-miR-145 was significantly reduced in extracts of *Ksrp*$^{-/-}$ eWAT (Fig. 6F). Addition of recombinant KSRP to *Ksrp*$^{-/-}$ extracts restored pre-miR-145 production (Fig. 6G). In contrast, processing of a control pri-miR-23b was equivalent between wild-type and *Ksrp*$^{-/-}$ eWAT (Fig. 6H). These data suggest that decreased miR-145 expression in *Ksrp*$^{-/-}$ eWAT is indeed due to a reduction in pri-miR-145 processing.

Downregulation of KSRP in 3T3-L1 adipocytes enhances lipolysis and reduces miR-145 expression. To determine the molecular mechanism that lead to enhanced lipolysis, we used an *in vitro* adipocyte differentiation model of 3T3-L1 fibroblasts. 3T3-L1 cells were transfected with a control siRNA (siControl) or a KSRP siRNA (siKsrp). After differentiation, lipolysis and expression of lipolytic genes were analyzed. As the isoproterenol-stimulated condition resembles the fasting state, we also examined lipolytic gene expression under this condition. Downregulation of KSRP enhanced lipolysis (Fig. 7B and C) and increased *Pnpla2*, *Lipe*, *Foxo1*, and *Cgi58* mRNA levels (Fig. 7D) and FOXO1, CGI58, and ATGL protein levels (Fig. 7A) under both basal and stimulated conditions. While KSRP knockdown did not increase *Foxo1* mRNA levels under the basal condition (Fig. 7D), it increased the protein levels (Fig. 7A), suggesting that *Foxo1* translation was increased under this condition. In contrast, no difference in the expression of *Pparg* and *Fabp4* was observed upon KSRP knockdown (Fig. 7E), suggesting that KSRP is not required for adipogenesis of 3T3-L1 cells. Similar to the observation in *Ksrp*$^{-/-}$ eWAT, KSRP knockdown decreased miR-145 levels and increased pri-miR-145 levels under both basal and stimulated conditions (Fig. 7F). While fasting increased miR-145 levels in wild-type eWAT (Fig. 6A), its levels were not increased under the stimulated condition in siControl-treated 3T3-L1 adipocytes (Fig. 7F). This discrepancy is likely due to the differences in cell type and/or signaling pathways between isoproterenol-stimulated 3T3-L1 adipocytes and fasting-stimulating eWAT. These data indicate that elevated lipolysis, as well as decreased miR-145 expression, can be recapitulated in 3T3-L1 adipocytes upon KSRP downregulation.

Overexpression of KSRP reduces FOXO1 and CGI58 and lipolysis and increases miR-145 expression. We next examined whether overexpression of KSRP attenuates lipolysis. Ectopic expression of FLAG-KSRP in 3T3-L1 adipocytes decreased the expression of FOXO1 and CGI58 (Fig. 8A) and increased the levels of miR-145 (Fig. 8B) under both basal and stimulated conditions. As a result of the increase in miR-145, pri-miR-145 levels were moderately decreased (Fig. 8C). More importantly, basal and stimulated lipolysis was significantly attenuated by KSRP overexpression (Fig. 8D). These results indicate that KSRP induces miR-145 expression by promoting pri-miR-145 processing, which decreases the levels of FOXO1 and CGI58 and lipolysis.

Ectopic expression of miR-145 attenuates lipolysis, and miR-145 directly targets *Foxo1* and *Cgi58*. To determine the role of miR-145 in controlling lipolytic gene expression and lipolysis, we

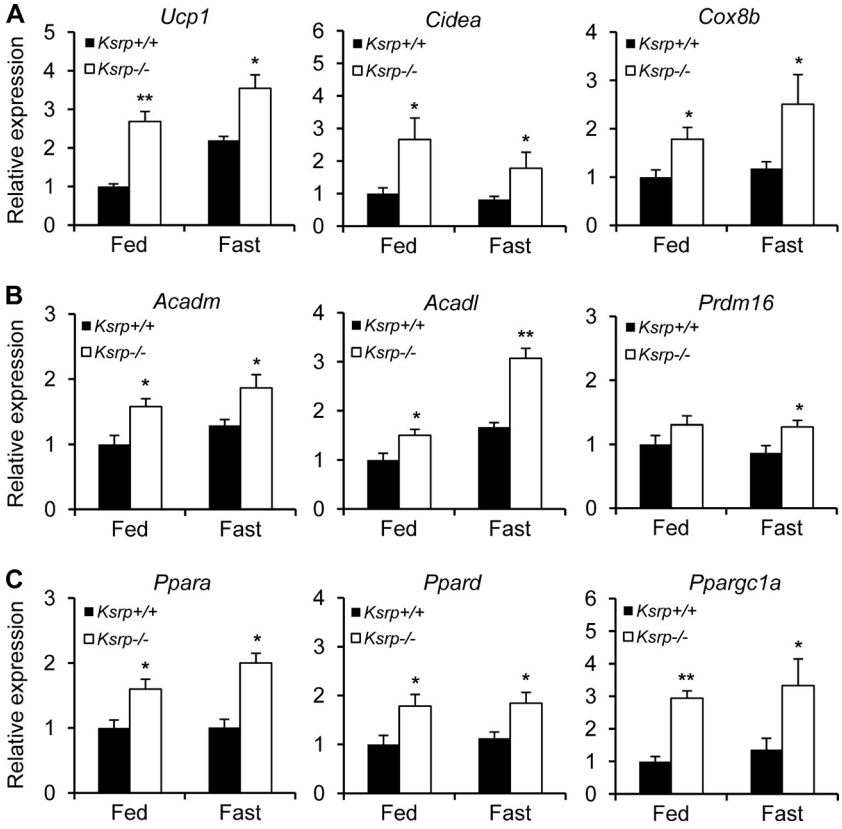

FIG 5 Increased expression of genes involved in thermogenesis and fatty acid oxidation in *Ksrp*$^{-/-}$ eWAT. (A) Expression of *Ucp1*, *Cidea*, and *Cox8b* was analyzed by qPCR in eWAT of fed or fasted wild-type ($n = 8$) and *Ksrp*$^{-/-}$ ($n = 8$) mice. (B) Expression of *Acadm*, *Acadl*, and *Prdm16* was analyzed by qPCR in eWAT of fed or fasted wild-type and *Ksrp*$^{-/-}$ mice. (C) Expression of *Ppara*, *Ppard*, and *Ppargc1a* was analyzed by qPCR in the eWAT of fed or fasted wild-type and *Ksrp*$^{-/-}$ mice. The expression of each gene in fed wild-type mouse eWAT was set at 1. Data are mean ± SEM. *, $P < 0.05$; **, $P < 0.01$.

overexpressed miR-145 in 3T3-L1 cells transfected with either siControl or siKsrp. Forced expression of miR-145 decreased *Pnpla2*, *Lipe*, *Foxo1*, and *Cgi58* (Fig. 9A) but not *Fabp4* (Fig. 9B) mRNA levels and FOXO1 and CGI58 protein levels (Fig. 9C) in siControl- and siKsrp-treated adipocytes under both basal and stimulated conditions. Accordingly, ectopic miR-145 expression repressed lipolysis in 3T3-L1 adipocytes treated with siControl and siKsrp under both basal and stimulated conditions (Fig. 9D).

Bioinformatics analysis predicted that *Foxo1* and *Cgi58* are targets of miR-145, with each 3′ UTR containing a potential target site (Fig. 9E). To verify that miR-145 can directly target *Foxo1* and *Cgi58* mRNAs, we subcloned their 3′ UTRs into a dual-luciferase reporter. Expression of miR-145 decreased the expression of luciferase reporters harboring the 3′ UTRs of *Foxo1* and *Cgi58* but not that of a control reporter, MT01, without an insertion (Fig. 9F). Mutations of the target sites in *Foxo1* and *Cgi58* resisted inhibition by miR-145 (Fig. 9F). Altogether, these data indicate that miR-145 directly regulates the expression of *Foxo1* and *Cgi58*, leading to changes in the expression of *Pnpla2* and *Lipe* and ATGL activity, thus lipolysis.

Downregulation of *Foxo1* and *Cgi58* attenuates lipolysis. To determine whether elevated lipolysis in the absence of KSRP is due to increased expression of *Foxo1* and *Cgi58*, we downregulated their expression by siRNAs in 3T3-L1 adipocytes treated with either siControl or siKsrp. Downregulation of *Foxo1* and *Cgi58* decreased lipolysis in both siControl- and siKsrp-treated adipocytes under both basal and stimulated conditions (Fig. 10A). These data indicate that the increase in lipolysis in 3T3-L1 adipocytes upon the downregulation of KSRP is indeed due to increased expression of *Foxo1* and *Cgi58*.

DISCUSSION

This study shows that targeted deletion of KSRP enhances lipolysis in eWAT through the elevated expression of *Foxo1* and *Cgi58*. We demonstrated that KSRP is involved in the processing of pri-miR-145 in eWAT and that its absence results in the downregulation of miR-145. Mechanistically, miR-145 directly represses *Foxo1* and *Cgi58*. Thus, reduction of miR-145 levels in *Ksrp*$^{-/-}$ eWAT leads to derepression of these genes, thereby increasing lipolysis. These findings suggest that KSRP is a critical factor for balancing TAG storage and hydrolysis in white adipocytes and that its absence favors hydrolysis partly through the posttranscriptional regulation of miR-145 expression.

FOXO1 is a transcriptional activator of *Pnpla2* and stimulates lipolysis (8). It is also required for fasting-induced expression of *Irf4*, which activates the expression of *Pnpla2* and *Lipe* (9). Thus, elevated expression of *Irf4*, *Pnpla2*, and *Lipe* in *Ksrp*$^{-/-}$ eWAT is likely due to increased FOXO1. CGI58 (ABHD5) interacts with ATGL and stimulates its TAG hydrolase activity (10). Using adipocytes derived from 3T3-L1 cells, we demonstrated that ectopic expression of miR-145 attenuates *Foxo1* and *Cgi58*, as well as lipolysis, and downregulation of *Foxo1* and *Cgi58* attenuates lipol-

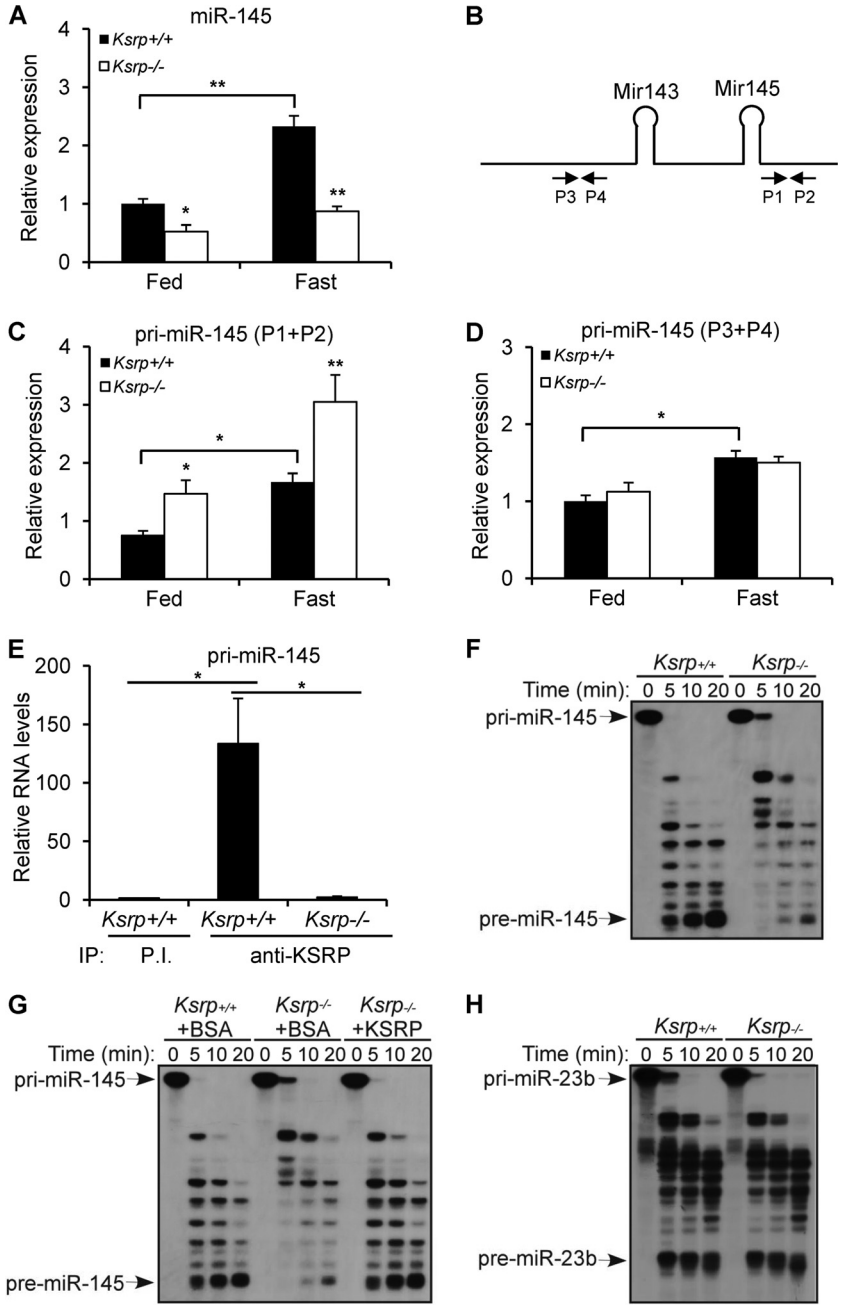

FIG 6 Decreased miR-145 expression in *Ksrp*$^{-/-}$ eWAT resulting from impaired pri-miRNA processing. (A) Levels of miR-145 were analyzed by qPCR in eWAT of fed or fasted wild-type ($n = 8$) and *Ksrp*$^{-/-}$ ($n = 8$) mice. The level in fed wild-type mice was set at 1. Data are mean ± SEM. *, $P < 0.05$; **, $P < 0.01$. (B) Schematic diagram showing the organization of Mir143 and Mir145 and the locations of primers for qPCR. (C and D) Pri-miR-143 and -145 levels in eWAT of fed or fasted wild-type ($n = 8$) and *Ksrp*$^{-/-}$ ($n = 8$) mice were analyzed by qPCR with P1 and P2 (C) or P3 and P4 (D). Data are mean ± SEM. *, $P < 0.05$; **, $P < 0.01$. (E) Association of pri-miR-145 with KSRP. Extracts of wild-type and *Ksrp*$^{-/-}$ eWAT were immunoprecipitated (IP) with a control serum or anti-KSRP serum and anti-KSRP serum, respectively. Pri-miR-145 transcripts in the precipitates were analyzed by qPCR. Data are mean ± SEM of three independent experiments. *, $P < 0.05$. P.I., preimmune serum. (F) *In vitro* pri-miR-145 processing with extracts of wild-type or *Ksrp*$^{-/-}$ eWAT. (G) *In vitro* pri-miR-145 processing with extracts of wild-type or *Ksrp*$^{-/-}$ eWAT in the absence or presence of recombinant KSRP. (H) *In vitro* pri-miR-23b processing with extracts of wild-type or *Ksrp*$^{-/-}$ eWAT.

ysis. These data strongly suggest that enhanced lipolysis in *Ksrp*$^{-/-}$ eWAT is due to elevated expression of *Foxo1* and *Cgi58*, leading to increased expression of *Pnpla2*, as well as elevated ATGL activity, and identify a novel function of miR-145 in controlling lipolysis in WAT.

A recent study showed that adipose-tissue-selective overexpression of CGI58 (ABHD5) did not increase lipolysis or protect against diet-induced obesity (24), suggesting that the expression of CGI58 in mouse adipose tissue is not limiting for either basal or stimulated lipolysis. These findings are somewhat contradictory to our hypothesis that increased CGI58 in *Ksrp*$^{-/-}$ eWAT leads to enhanced lipolysis. It is possible that ATGL levels are also

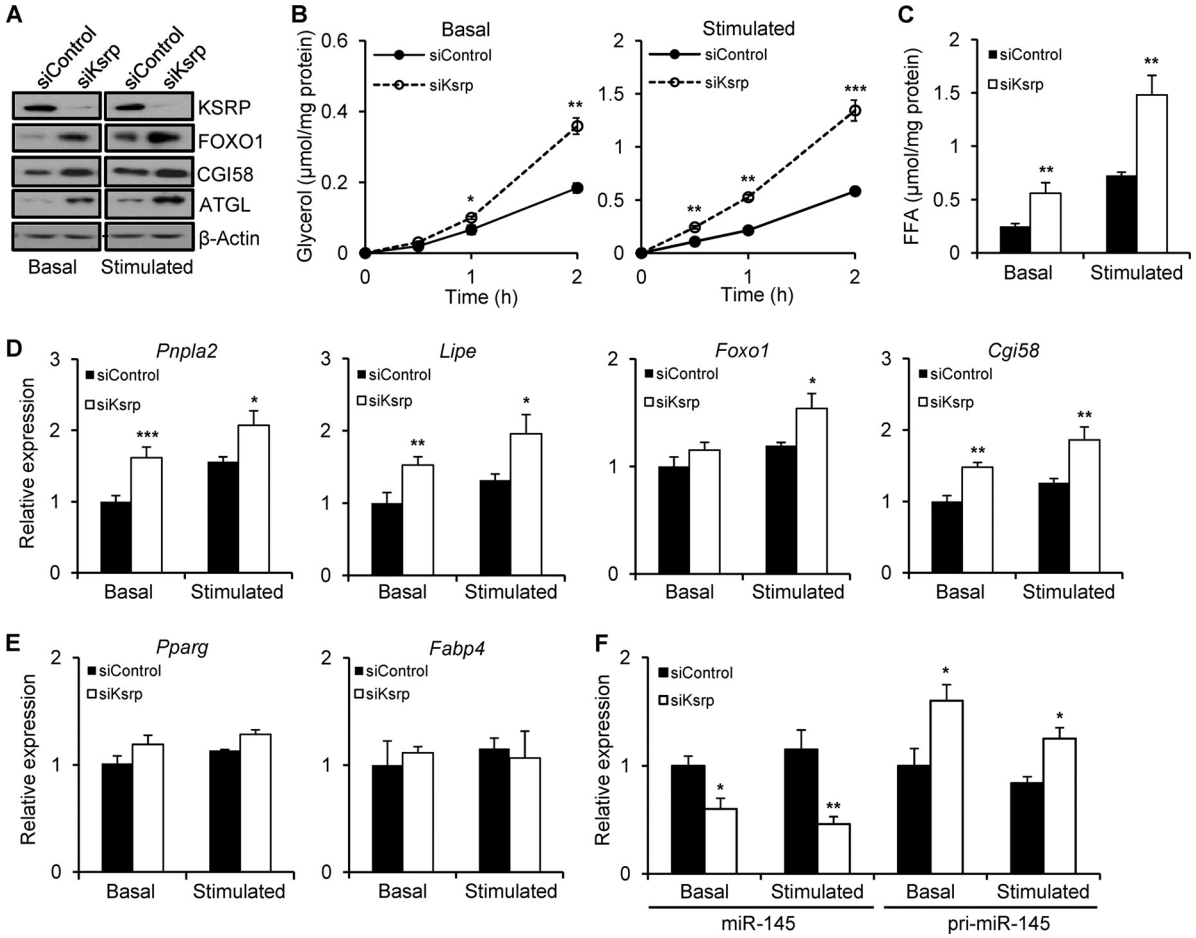

FIG 7 Enhanced lipolysis and lipolytic gene expression, reduced miR-145 levels, and increased pri-miR-145 levels in 3T3-L1 adipocytes upon downregulation of KSRP. (A) 3T3-L1 cells were transfected with siControl or siKsrp and induced for differentiation for 5 days. KSRP, FOXO1, CGI58, ATGL, and β-actin levels were analyzed by immunoblotting under both basal and stimulated conditions. (B and C) Glycerol (B) and FA (C) release was measured in the absence or presence of isoproterenol. FFA, free FA. (D) *Pnpla2*, *Lipe*, *Foxo1*, and *Cgi58* expression was analyzed under both basal and stimulated conditions. (E) *Pparg* and *Fabp4* expression was analyzed under both basal and stimulated conditions. (F) miR-145 and pri-miR-145 levels were analyzed under both basal and stimulated conditions. The expression of each gene in siControl-treated adipocytes under the basal condition was set at 1. Data are mean ± SEM from two independent experiments. *, $P < 0.05$; **, $P < 0.01$; ***, $P < 0.001$.

limiting in adipose tissue, which explains that a further increase in CGI58 levels did not enhance ATGL activity, as well as lipolysis, in the study (24). However, we found that both ATGL and CGI58 levels were increased in the absence of KSRP (Fig. 3B and 7A). Hence, we suggest that simultaneous increases in the levels of ATGL and CGI58 result in elevated lipolysis in *Ksrp*$^{-/-}$ eWAT, consistent with the previous finding that CGI58 activates ATGL activity (10).

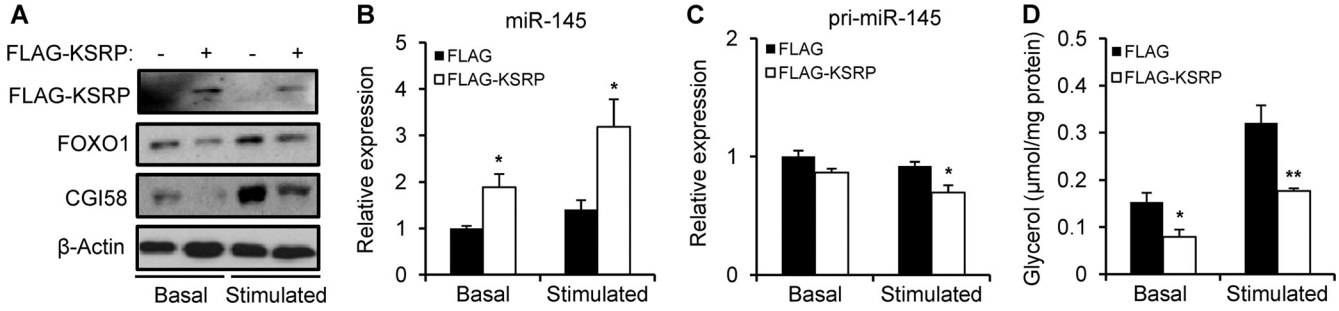

FIG 8 Overexpression of KSRP upregulates miR-145 and attenuates lipolysis. (A) 3T3-L1 cells were transfected with a control vector or a vector expressing FLAG-KSRP and induced for differentiation for 5 days. FLAG-KSRP, FOXO1, CGI58, and β-actin levels were analyzed by immunoblotting under both basal and stimulated conditions. (B and C) miR-145 (B) and pri-miR-145 (C) levels were analyzed under both basal and stimulated conditions. (D) Glycerol release was measured in the absence or presence of isoproterenol for 2 h. Data are mean ± SEM ($n = 4$). *, $P < 0.05$; **, $P < 0.01$.

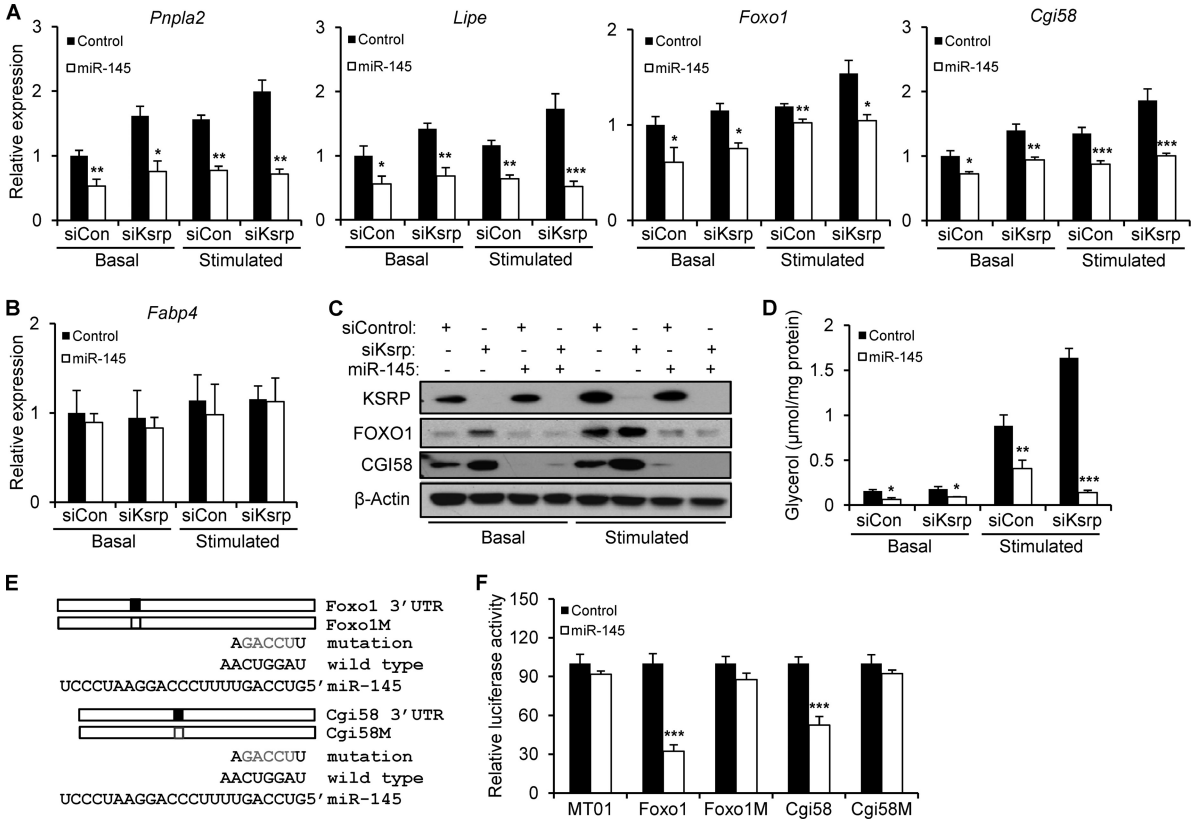

FIG 9 Repression of lipolytic genes and lipolysis by ectopic expression of miR-145 and miR-145 directly targets *Foxo1* and *Cgi58*. (A and B) *Pnpla2*, *Lipe*, *Foxo1*, *Cgi58* (A), and *Fabp4* (B) expression was analyzed in 3T3-L1 adipocytes transfected with control or miR-145 mimics and siControl (siCon) or siKsrp under both basal and stimulated conditions. The expression of each gene in siControl-treated adipocytes under the basal condition was set at 1. (C) KSRP, FOXO1, CGI58, and β-actin levels were analyzed by immunoblotting under both basal and stimulated conditions. (D) Glycerol release was measured under both basal and stimulated conditions. (E) Schematic diagrams showing the 3′ UTRs of *Foxo1* and *Cgi58*. miR-145 target sites and mutations in the seed motif. (F) Relative luciferase activities in NIH 3T3 cells cotransfected with reporter constructs and a control mimic or a miR-145 mimic. Data are mean ± SEM from two independent experiments. *, $P < 0.05$; **, $P < 0.01$; ***, $P < 0.001$.

We found that pri-miR-145 and miR-145 but not KSRP levels were increased during fasting in wild-type eWAT (Fig. 6A and C and Fig. 3B). These data suggest that the increase in miR-145 levels is due primarily to fasting-induced synthesis of pri-miR145, although we cannot exclude the possibility that the pri-miRNA processing activity of KSRP is also increased during fasting. As fasting increases lipolysis and induces miR-145, which is a negative regulator of lipolysis, we suggest that miR-145 serves as a negative

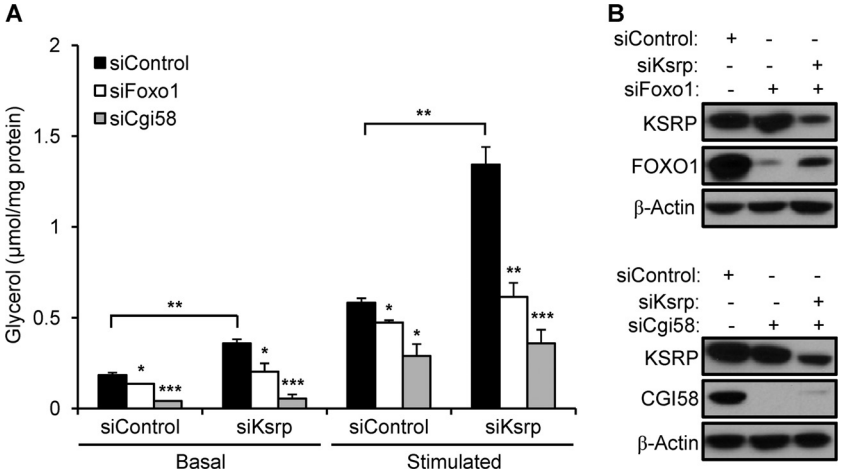

FIG 10 Downregulation of *Foxo1* and Cgi58 attenuates lipolysis. (A) Glycerol release was measured in 3T3-L1 adipocytes transfected with siControl or siKsrp and si*Foxo1* or si*Cgi58* under both basal and stimulated conditions. Data are mean ± SEM from two independent experiments. *, $P < 0.05$; **, $P < 0.01$; ***, $P < 0.001$. (B) KSRP, FOXO1, CGI58, and β-actin levels were analyzed by immunoblotting.

feedback factor to prevent uncontrolled lipolysis during times of demand, such as fasting.

While we have focused entirely on the regulation of FOXO1 and CGI58 by miR-145 in the present study, it is likely that miR-145 also represses other factors that promote lipolysis. Further analysis of miR-145 targets in eWAT should result in the identification of such factors. We also observed the upregulation of genes involved in thermogenesis and mitochondrial FA oxidation in *Ksrp*$^{-/-}$ eWAT. This upregulation may be due directly to reduced miR-145 expression or result indirectly from increasing lipolysis, which has been shown to increase the expression of these genes (2, 3). Our preliminary analysis showed that overexpression of miR-145 in 3T3-L1 adipocytes repressed the expression of *Prdm16*, *Ppara*, *Ppard*, *Ppargc1a*, and fatty acid oxidation genes. Interestingly, *Prdm16*, *Ppara*, and *Ppard* are predicted targets of miR-145. Thus, upregulation of these genes in *Ksrp*$^{-/-}$ eWAT (Fig. 5) is likely due to reduced miR-145 expression. It is also possible that KSRP directly regulates the expression of mRNAs that encode transcriptional regulators critical for fat utilization in eWAT, such as peroxisome proliferator-activated receptor α (PPARα), PPARδ, or PPRAGC1α, through other posttranscriptional mechanisms.

Whereas KSRP has been shown to be required for the processing of a subset of pri-miRNAs in several models of established cell lines through RNA interference-induced downregulation (14, 25), it is somewhat surprising to find that only miR-145 is reduced in *Ksrp*$^{-/-}$ eWAT by microarray analysis. Other miRNAs previously shown to be regulated by KSRP did not show a difference in *Ksrp*$^{-/-}$ eWAT in our analysis, although they are clearly expressed in eWAT (data not shown). It is unclear why only miR-145 expression is decreased in eWAT while other KSRP-dependent miRNAs are not. Our findings, together with previous reports (14, 19, 25, 26), suggest a possible cell type or tissue specificity for KSRP-dependent pri-miRNA processing. The function of KSRP in pri-miRNA processing is also likely compensated by its close family members, including FBP1 and FBP3 (27), depending on the cell type. Furthermore, the mechanism by which KSRP promotes pri-miR-145 processing awaits further investigation, although previous data suggest that it interacts with the terminal loop of pre-miRNAs.

While *Ksrp*$^{-/-}$ mice have a reduced fat mass, it will be of interest to see whether the enhanced lipolysis and fatty acid utilization in WAT are the sole contributions to this phenotype. We also found that *Ksrp*$^{-/-}$ mice exhibited a reduced body weight, increased expression of brown-fat-selective genes in inguinal WAT, and moderately increased energy expenditure while no differences in activity or food intake were observed (31). These data suggest that the reduction in body adiposity is likely due to increased FA utilization in white adipose tissue. Further studies with adipose-tissue-specific KSRP knockout mice should reveal its role in the control of lipolysis and whole-body adiposity. Nevertheless, our observations are consistent with previous findings that increasing lipolysis in WAT promotes FA oxidation within adipocytes and protects against obesity (2, 3, 23, 28–30). It will also be of interest to examine whether gain- and loss-of-function of miR-145 in adipose tissue affect lipolysis and adiposity *in vivo*. In summary, this work suggests that modulation of KSRP-dependent pri-miR-145 processing could be a potential therapeutic target for obesity and metabolic disorders.

ACKNOWLEDGMENTS

This work was supported by NIH grant GM068758 (C.-Y.C.) and grants from the Ministero della Salute (RF-2010-2306205) and AICR (10-0527) to R.G.

REFERENCES

1. **Duncan RE, Ahmadian M, Jaworski K, Sarkadi-Nagy E, Sul HS.** 2007. Regulation of lipolysis in adipocytes. Annu. Rev. Nutr. **27:**79–101. http://dx.doi.org/10.1146/annurev.nutr.27.061406.093734.
2. **Ahmadian M, Duncan RE, Varady KA, Frasson D, Hellerstein MK, Birkenfeld AL, Samuel VT, Shulman GI, Wang Y, Kang C, Sul HS.** 2009. Adipose overexpression of desnutrin promotes fatty acid use and attenuates diet-induced obesity. Diabetes **58:**855–866. http://dx.doi.org/10.2337/db08-1644.
3. **Jaworski K, Ahmadian M, Duncan RE, Sarkadi-Nagy E, Varady KA, Hellerstein MK, Lee HY, Samuel VT, Shulman GI, Kim KH, de Val S, Kang C, Sul HS.** 2009. AdPLA ablation increases lipolysis and prevents obesity induced by high-fat feeding or leptin deficiency. Nat. Med. **15:**159–168. http://dx.doi.org/10.1038/nm.1904.
4. **Villena JA, Roy S, Sarkadi-Nagy E, Kim KH, Sul HS.** 2004. Desnutrin, an adipocyte gene encoding a novel patatin domain-containing protein, is induced by fasting and glucocorticoids: ectopic expression of desnutrin increases triglyceride hydrolysis. J. Biol. Chem. **279:**47066–47075. http://dx.doi.org/10.1074/jbc.M403855200.
5. **Schweiger M, Schreiber R, Haemmerle G, Lass A, Fledelius C, Jacobsen P, Tornqvist H, Zechner R, Zimmermann R.** 2006. Adipose triglyceride lipase and hormone-sensitive lipase are the major enzymes in adipose tissue triacylglycerol catabolism. J. Biol. Chem. **281:**40236–40241. http://dx.doi.org/10.1074/jbc.M608048200.
6. **Zimmermann R, Strauss JG, Haemmerle G, Schoiswohl G, Birner-Gruenberger R, Riederer M, Lass A, Neuberger G, Eisenhaber F, Hermetter A, Zechner R.** 2004. Fat mobilization in adipose tissue is promoted by adipose triglyceride lipase. Science **306:**1383–1386. http://dx.doi.org/10.1126/science.1100747.
7. **Haemmerle G, Zimmermann R, Hayn M, Theussl C, Waeg G, Wagner E, Sattler W, Magin TM, Wagner EF, Zechner R.** 2002. Hormone-sensitive lipase deficiency in mice causes diglyceride accumulation in adipose tissue, muscle, and testis. J. Biol. Chem. **277:**4806–4815. http://dx.doi.org/10.1074/jbc.M110355200.
8. **Chakrabarti P, Kandror KV.** 2009. FoxO1 controls insulin-dependent adipose triglyceride lipase (ATGL) expression and lipolysis in adipocytes. J. Biol. Chem. **284:**13296–13300. http://dx.doi.org/10.1074/jbc.C800241200.
9. **Eguchi J, Wang X, Yu S, Kershaw EE, Chiu PC, Dushay J, Estall JL, Klein U, Maratos-Flier E, Rosen ED.** 2011. Transcriptional control of adipose lipid handling by IRF4. Cell Metab. **13:**249–259. http://dx.doi.org/10.1016/j.cmet.2011.02.005.
10. **Lass A, Zimmermann R, Haemmerle G, Riederer M, Schoiswohl G, Schweiger M, Kienesberger P, Strauss JG, Gorkiewicz G, Zechner R.** 2006. Adipose triglyceride lipase-mediated lipolysis of cellular fat stores is activated by CGI-58 and defective in Chanarin-Dorfman Syndrome. Cell Metab. **3:**309–319. http://dx.doi.org/10.1016/j.cmet.2006.03.005.
11. **Yang X, Lu X, Lombes M, Rha GB, Chi YI, Guerin TM, Smart EJ, Liu J.** 2010. The G(0)/G(1) switch gene 2 regulates adipose lipolysis through association with adipose triglyceride lipase. Cell Metab. **11:**194–205. http://dx.doi.org/10.1016/j.cmet.2010.02.003.
12. **Min H, Turck CW, Nikolic JM, Black DL.** 1997. A new regulatory protein, KSRP, mediates exon inclusion through an intronic splicing enhancer. Genes Dev. **11:**1023–1036. http://dx.doi.org/10.1101/gad.11.8.1023.
13. **Gherzi R, Lee KY, Briata P, Wegmuller D, Moroni C, Karin M, Chen CY.** 2004. A KH domain RNA binding protein, KSRP, promotes ARE-directed mRNA turnover by recruiting the degradation machinery. Mol. Cell **14:**571–583. http://dx.doi.org/10.1016/j.molcel.2004.05.002.
14. **Trabucchi M, Briata P, Garcia-Mayoral M, Haase AD, Filipowicz W, Ramos A, Gherzi R, Rosenfeld MG.** 2009. The RNA-binding protein KSRP promotes the biogenesis of a subset of microRNAs. Nature **459:**1010–1014. http://dx.doi.org/10.1038/nature08025.
15. **Dhamija S, Kuehne N, Winzen R, Doerrie A, Dittrich-Breiholz O, Thakur BK, Kracht M, Holtmann H.** 2011. Interleukin-1 activates synthesis of interleukin-6 by interfering with a KH-type splicing regulatory

protein (KSRP)-dependent translational silencing mechanism. J. Biol. Chem. **286:**33279–33288. http://dx.doi.org/10.1074/jbc.M111.264754.
16. **Chen CY, Gherzi R, Ong SE, Chan EL, Raijmakers R, Pruijn GJ, Stoecklin G, Moroni C, Mann M, Karin M.** 2001. AU binding proteins recruit the exosome to degrade ARE-containing mRNAs. Cell **107:**451–464. http://dx.doi.org/10.1016/S0092-8674(01)00578-5.
17. **Lin WJ, Zheng X, Lin CC, Tsao J, Zhu X, Cody JJ, Coleman JM, Gherzi R, Luo M, Townes TM, Parker JN, Chen CY.** 2011. Posttranscriptional control of type I interferon genes by KSRP in the innate immune response against viral infection. Mol. Cell. Biol. **31:**3196–3207. http://dx.doi.org/10.1128/MCB.05073-11.
18. **Soukas A, Socci ND, Saatkamp BD, Novelli S, Friedman JM.** 2001. Distinct transcriptional profiles of adipogenesis in vivo and in vitro. J. Biol. Chem. **276:**34167–34174. http://dx.doi.org/10.1074/jbc.M104421200.
19. **Briata P, Lin WJ, Giovarelli M, Pasero M, Chou CF, Trabucchi M, Rosenfeld MG, Chen CY, Gherzi R.** 2012. PI3K/AKT signaling determines a dynamic switch between distinct KSRP functions favoring skeletal myogenesis. Cell Death Differ. **19:**478–487. http://dx.doi.org/10.1038/cdd.2011.117.
20. **Pasero M, Giovarelli M, Bucci G, Gherzi R, Briata P.** 2012. Bone morphogenetic protein/SMAD signaling orients cell fate decision by impairing KSRP-dependent microRNA maturation. Cell Rep. **2:**1159–1168. http://dx.doi.org/10.1016/j.celrep.2012.10.020.
21. **Hall MP, Huang S, Black DL.** 2004. Differentiation-induced colocalization of the KH-type splicing regulatory protein with polypyrimidine tract binding protein and the c-src pre-mRNA. Mol. Biol. Cell **15:**774–786. http://dx.doi.org/10.1091/mbc.E03-09-0692.
22. **Rangwala SM, Rhoades B, Shapiro JS, Rich AS, Kim JK, Shulman GI, Kaestner KH, Lazar MA.** 2003. Genetic modulation of PPARgamma phosphorylation regulates insulin sensitivity. Dev. Cell **5:**657–663. http://dx.doi.org/10.1016/S1534-5807(03)00274-0.
23. **Liew CW, Boucher J, Cheong JK, Vernochet C, Koh HJ, Mallol C, Townsend K, Langin D, Kawamori D, Hu J, Tseng YH, Hellerstein MK, Farmer SR, Goodyear L, Doria A, Bluher M, Hsu SI, Kulkarni RN.** 2013. Ablation of TRIP-Br2, a regulator of fat lipolysis, thermogenesis and oxidative metabolism, prevents diet-induced obesity and insulin resistance. Nat. Med. **19:**217–226. http://dx.doi.org/10.1038/nm.3056.
24. **Caviglia JM, Betters JL, Dapito DH, Lord CC, Sullivan S, Chua S, Yin T, Sekowski A, Mu H, Shapiro L, Brown JM, Brasaemle DL.** 2011. Adipose-selective overexpression of ABHD5/CGI-58 does not increase lipolysis or protect against diet-induced obesity. J. Lipid Res. **52:**2032–2042. http://dx.doi.org/10.1194/jlr.M019117.
25. **Zhang X, Wan G, Berger FG, He X, Lu X.** 2011. The ATM kinase induces microRNA biogenesis in the DNA damage response. Mol. Cell **41:**371–383. http://dx.doi.org/10.1016/j.molcel.2011.01.020.
26. **Ruggiero T, Trabucchi M, De Santa F, Zupo S, Harfe BD, McManus MT, Rosenfeld MG, Briata P, Gherzi R.** 2009. LPS induces KH-type splicing regulatory protein-dependent processing of microRNA-155 precursors in macrophages. FASEB J. **23:**2898–2908. http://dx.doi.org/10.1096/fj.09-131342.
27. **Davis-Smyth T, Duncan RC, Zheng T, Michelotti G, Levens D.** 1996. The far upstream element-binding proteins comprise an ancient family of single-strand DNA-binding transactivators. J. Biol. Chem. **271:**31679–31687. http://dx.doi.org/10.1074/jbc.271.49.31679.
28. **Nishino N, Tamori Y, Tateya S, Kawaguchi T, Shibakusa T, Mizunoya W, Inoue K, Kitazawa R, Kitazawa S, Matsuki Y, Hiramatsu R, Masubuchi S, Omachi A, Kimura K, Saito M, Amo T, Ohta S, Yamaguchi T, Osumi T, Cheng J, Fujimoto T, Nakao H, Nakao K, Aiba A, Okamura H, Fushiki T, Kasuga M.** 2008. FSP27 contributes to efficient energy storage in murine white adipocytes by promoting the formation of unilocular lipid droplets. J. Clin. Invest. **118:**2808–2821. http://dx.doi.org/10.1172/JCI34090.
29. **Martinez-Botas J, Anderson JB, Tessier D, Lapillonne A, Chang BH, Quast MJ, Gorenstein D, Chen KH, Chan L.** 2000. Absence of perilipin results in leanness and reverses obesity in Lepr(db/db) mice. Nat. Genet. **26:**474–479. http://dx.doi.org/10.1038/82630.
30. **Tansey JT, Sztalryd C, Gruia-Gray J, Roush DL, Zee JV, Gavrilova O, Reitman ML, Deng CX, Li C, Kimmel AR, Londos C.** 2001. Perilipin ablation results in a lean mouse with aberrant adipocyte lipolysis, enhanced leptin production, and resistance to diet-induced obesity. Proc. Natl. Acad. Sci. U. S. A. **98:**6494–6499. http://dx.doi.org/10.1073/pnas.101042998.
31. **Chou CF, Lin YY, Wang HK, Zhu X, Giovarelli M, Briata P, Gherzi R, Garvey WT, Chen CY.** 10 April 2014. KSRP ablation enhances brown fat gene program in white adipose tissue through reduced miR-150 expression. Diabetes http://dx.doi.org/10.2337/db13-1901.